SPECKLE NOISE REDUCTION IN ULTRASOUND IMAGES

Apexa V. Durve[1],Ketki C. Pathak[2]
Research Scholar[1], Associate Proffessor[2],
Department of Electronics & Communication,
Sarvajanik College of Engineering & technology,Surat.
Gujarat,India.
Email: apexadurve@gmail.com[1], ketki.joshi@scet.ac.in[2]

Abstract—Speckle noise is an inherent characteristic of any coherent imaging modality. It generally decreases the picture resolution and contrast, and therefore diagnostic value of image also reduces. So, speckle noise reduction is a very important prerequisite step before processing ultrasound images for further processing like segmentation and registration. There are many speckle noise reduction techniques in the literature like filtering, transform domain and statistical approach. But in terms of robustness and accuracy Speckle Reducing Anisotropic Diffusion which is Partial Differential Equation based approach performs better compared to others and they use instantaneous coefficient of variation to enhance the edge information. Results are tested on different ultrasound images of abdomen, kidney, brest and carotid artery using local statistics approach like Lee, Frost and Kuan and partial differential equation based approach like SRAD among which SRAD performs better in terms of PSNR and SSIM for different ultrasound images.

Index Terms—Ultrasound Imaging, Lee Filter, Frost Filter, Kuan Filter, Diffusion Filtering

I. INTRODUCTION

Medical ultrasound is a very important imaging modality in the clinical applications. Compared to other imaging modalities such as X-ray, magnetic resonance imaging (MRI), computed tomography (CT) and positron emission tomography (PET), diagnostic ultrasound imaging owes its great popularity to the fact that it is a safe and non invasive procedure for visualizing interior of the body. Other advantages of this ultrasound imaging technique are real time imaging capabilities, accessibility and a relatively low cost.

However, medical ultrasound imaging suffers from speckle noise which generally tends to reduce the image resolution and contrast, thereby reducing the diagnostic value of this imaging modality. Speckle is a granular pattern formed from constructive and destructive interferences of backscattered ultrasound waves. Speckle has been considered an undesirable noise source and techniques have been developed to minimize its effects.

The speckle pattern, which is visible as the typical light, and dark spots the image is composed of, results from constructive and destructive interference of ultrasound waves scattered from different sites.

II. SPECKLE IN MEDICAL ULTRASOUND IMAGING

A. *Speckle Modelling*

In medical ultrasound imaging, a speckle pattern is formed due to constructive and destructive interferences of backscattered echoes from the scatterers that are typically much smaller than the wavelength of an ultrasound wave. It has been known that speckle has a multiplicative nature. Thus, the image containing speckle, r(x, y), can be represented by

$$r(x, y) = h(x, y)n_m(x, y) + n_a(x, y) \text{...........}(1.1)$$

Where, $h(x, y)$ is the noise-free image, $n_m(x, y)$ is the multiplicative noise (i.e., speckle) and $n_a(x, y)$ is the additive noise. By assuming that the additive noise (e.g., thermal and electronic noises) is trivial compared to the multiplicative speckle noise, Eq. 1.1 can be written as

$$r(x, y) = h(x, y)n_m(x, y) \text{............}(1.2)$$

III. IMPLEMENTED TECHNIQUES

A. *Local Statistics Filter*

These filters also make the assumption that the ratio of noise standard deviation to mean is constant throughout the image. This simplification is only strictly true in some situations. The spatially-varying mean and variance of the observed image are denoted $I(x, y)$ and $\sigma_I^{\,2}(x, y)$. The coefficients of variation of the image and noise are given as

$$C_I(x, y) = \frac{\sigma_I(x, y)}{I(x, y)}, C_n = \frac{\sigma_n}{n} \text{................}(2.1)$$

$c_I(x, y)$ is known to be an effective descriptor of textural information and image homogeneity. The filters in this section operate as a test based on this descriptor. In this evaluation estimate $c_n^{\,2}$ as the median of $c_I^{\,2}(x, y)$ over the image.

I. *Lee Filter*

The multiplicative Lee filter [7] approximates multiplicative noise with a linear model to obtain the signal estimate.

$$\hat{R}(x, y) = I(x, y)W(x, y) + \overline{I(x, y)}\{1 - W(x, y)\}$$

Where, W(x,y) is weighting function given by,

$$W(x, y) = 1 - \frac{C_n^{\,2}}{C_I^{\,2}(x, y)}$$

II. *Frost Filter*

In Frost [8] filter the noise-free image is obtained by convolving the observed image with a spatially-varying kernel as $\hat{R}(x, y) = I(x, y) * m(x, y)$. The kernel $m(x, y)$, centered at the pixel at location (x_0, y_0), is

$$m(x, y) = K_1 \exp(-KC_I^{\,2}(x_0, y_0)\left|x, y\right|) \text{..........}(2.4)$$

Where the dampening rate is controlled by K, |x, y| represents the distance of each pixel within the window to (x_0, y_0), and normalizing constant is denoted by K_1.

Parameter K must be chosen such that mean filtering is performed for homogeneous regions and filtering is inhibited at edges.

III. *Kuan Filter*

Instead of the linear approximation used in the Lee filter, the Kuan [9] filter is implemented by converting multiplicative noise into a signal dependant additive noise formulation. The general form is same as the Lee filter, but with a different weighting function which is given by

$$w(x, y) = \frac{1 - \dfrac{C_n^{\,2}}{C_I^{\,2}(x, y)}}{1 + C_n^{\,2}}$$

B. *Diffusion Techniques*

I. *Anisotropic Diffusion*

Anisotropic Diffusion[6] developed by Perona and Malik is a method of selectively smoothing an image while preserving edges. Diffusion takes place according to following partial differential equation (PDE):

$$\frac{\partial I}{\partial t} = div[c(\left|\nabla I\right|) \cdot \nabla I]$$

$$I(t = 0) = I_0$$

Where ∇ is the gradient operator, div the divergence operator, $|\;|$ denotes the magnitude, $c(x)$ the diffusion coefficient, and I_0 the initial image.

$$c(x) = \frac{1}{1 + (x / k)^2}$$

$$c(x) = \exp[-(x / k)^2]$$

Where, k is an edge magnitude parameter.

In the anisotropic diffusion method, the gradient magnitude is used to detect an image edge or boundary as a step discontinuity in intensity. If $\left|\nabla I\right| >> k$, then $c(\left|\nabla I\right|) \to 0$, and we have an all pass filter; if $\left|\nabla I\right| << k$, then $c(\left|\nabla I\right|) \to 1$, and we achieve isotropic diffusion (Gaussian filtering).

II. *Speckle Reducing Anisotropic Diffusion*

SRAD[3] is a Partial Differential Equation (PDE) approach to remove speckle noise from ultrasound images. The PDE based speckle removal approach allows the generation of an image scale space (a set of filtered images that varies from fine to coarse) without bias due to filter window size and shape.

The differential equation is numerically solved by using the iterative Jacobi method. Assuming a sufficiently small time step size and sufficiently small spatial step size of h in and directions, we discretize the time and space coordinates as follows:

$$t = n\Delta t, n = 0, 1, 2.....$$

$$x = ih, i = 0, 1, 2.......M - 1$$

$$y = jh, j = 0, 1, 2.......N - 1$$

Where, Size of the image support is given by $Mh \times Nh$.

Let $I_{i,j}^{\ n} = I(ih, jh, n\Delta t)$. To calculate the right hand side of the SRAD PDE we then use a three stage approach

In the first stage, we calculate the Laplacian and derivative approximations as:

$$\nabla_R I_{i,j}^{\ n} = [\frac{I_{i+1,j}^{\ n} - I_{i,j}^{\ n}}{h}, \frac{I_{i,j+1}^{\ n} - I_{i,j}^{\ n}}{h}]$$

$$\nabla_L I_{i,j}^{\ n} = [\frac{I_{i,j}^{\ n} - I_{i-1,j}^{\ n}}{h}, \frac{I_{i,j}^{\ n} - I_{i,j-1}^{\ n}}{h}]$$

$$\nabla^2 I_{i,j}^{\ n} = [\frac{I_{i+1,j}^{\ n} + I_{i-1,j}^{\ n} + I_{i,j+1}^{\ n} + I_{i,j-1}^{\ n} - 4I_{i,j}^{\ n}}{h^2}]$$

In the second stage, the diffusion coefficient $c(q)$ is given by following equation:

$$c_{i,j}^{\ n} = c[q\left(\frac{1}{I_{i,j}^{\ n}}\sqrt{\left|\nabla_R I_{i,j}^{\ n}\right|^2 + \left|\nabla_L I_{i,j}^{\ n}\right|^2}, \frac{1}{I_{i,j}^{\ n}}\nabla^2 I_{i,j}^{\ n}\right)]$$

Within the third stage, we calculate the divergence of $c(\cdot)\nabla I$, needed for the SRAD PDE as:

$$d_{i,j}^{\ n} = \frac{1}{h^2}[c_{i+1,j}^{\ n}(I_{i+1,j}^{\ n} - I_{i,j}^{\ n}) + c_{i,j}^{\ n}(I_{i-1,j}^{\ n} - I_{i,j}^{\ n})$$
$$+ c_{i,j+1}^{\ n}(I_{i,j+1}^{\ n} - I_{i,j}^{\ n}) + c_{i,j}^{\ n}(I_{i,j-1}^{\ n} - I_{i,j}^{\ n})] ..(3.10)$$

Finally, by approximating time derivative with forward differencing, the numerical approximation to the differential equation is given by:

$$I_{i,j}^{\ n+1} = I_{i,j}^{\ n} + \frac{\Delta t}{4} d_{i,j}^{\ n}$$

SRAD update equation is given by above equation. Choose $h = 1$ and $\Delta t = 0.05$ for numerical implementation. Moreover, since the diffusion coefficient will not be exactly equal to zero at any edge in a digital image, as an option, to better stop diffusion across main edges place $c_{i,j}^{\ n}$ to 0 if it is less than a lower threshold.

Hence, SRAD enhances edges by inhibiting diffusion across edges as well as preserves edges and allows diffusion on either side of the edge. It does not use hard thresholds to alter performance in homogeneous regions or in regions near edges and small features. SRAD is also adaptive in nature.

IV. RESULT ANALYSIS

Various speckle noise reduction techniques are implemented like Lee, Frost, Kuan, SRAD, DPAD and hybrid version of SRAD and DPAD on various data sets of abdomen, brest, carotid artery and kidney images which were taken from two different hospitals. Images of kidney were given by Dr.Umesh Udapudi who is radiologist in Udapudi Clinic and other images of abdomen, berst and carotid artery were taken from Dr.Mishra who is aradiologist in SMIMMER hospital, Surat. These images were in clean form. Images were degraded by adding speckle noise manually from MATLAB command imnoise for different noise variances and effect of noise removal filter was observed.

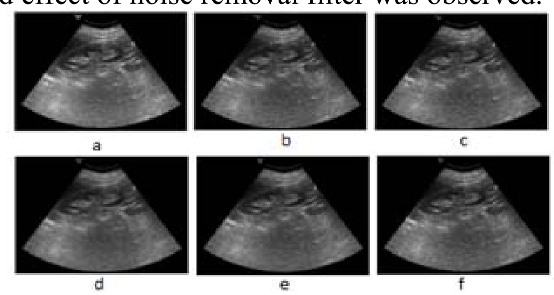

Figure 1(a)Original Image of abdomen (b)Noisy image with variance 0.02 (c) Lee filter (d) Frost filter (e) Kuan filter (f)SRAD filter

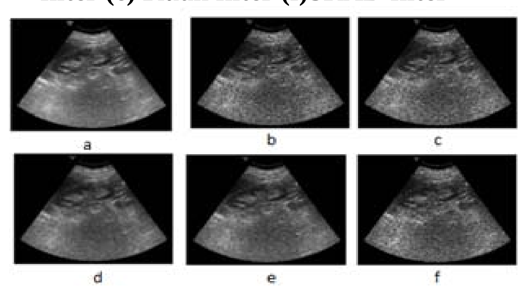

Figure 2(a)Original Image of abdomen(b)Noisy image with variance 0.2 (c) Lee filter (d) Frost filter (e) Kuan filter (f)SRAD filter

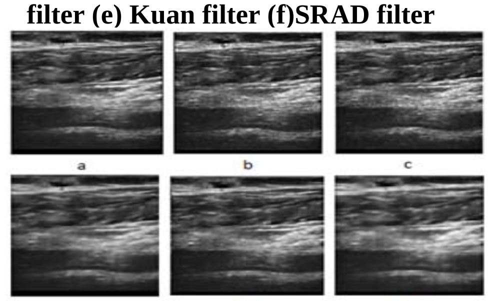

Figure 3(a)Original Image of brest (b)Noisy image with variance 0.02 (c) Lee filter (d) Frost filter (e) Kuan filter (f)SRAD filter

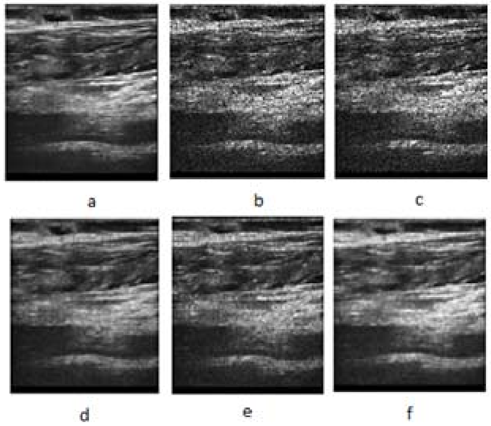

Figure 4(a)Original Image of brest(b)Noisy image with variance 0.2 (c) Lee filter (d) Frost filter (e) Kuan filter (f)SRAD filter

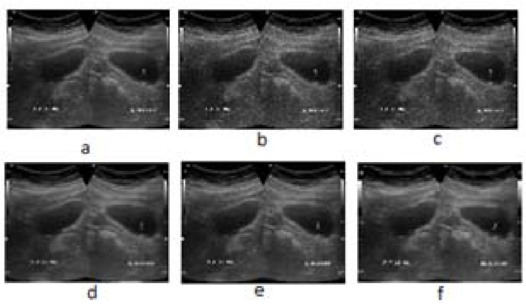

Figure 5(a)Original Image of kidney(b)Noisy image with variance 0.02 (c) Lee filter (d) Frost filter (e) Kuan filter (f)SRAD filter

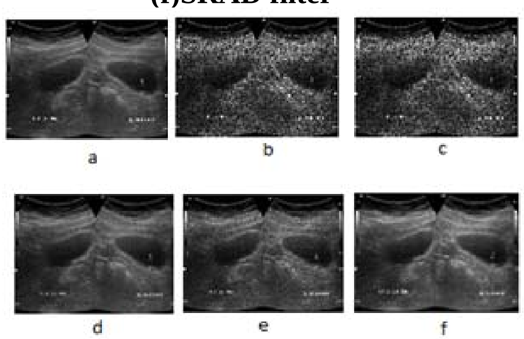

Figure 6(a)Original Image of kidney(b)Noisy image with variance 0.2 (c) Lee filter (d) Frost filter (e) Kuan filter (f)SRAD filter

V. PERFORMANCE MEASUREMENTS PARAMETERS

A. PSNR

MSE is defined as the average of square of the error where error is the difference between desired quantity and estimated quantity. The MSE provides a means of choosing the best estimator. Having a Mean Square Error of zero (0) is ideal. The MSE is defined as:

$$MSE = \frac{1}{MN}\sum_{x=0}^{M-1}\sum_{y=0}^{N-1}[f(x,y) - \hat{f}(x,y)]^2$$

Where f(x,y) is the original image and (x,y) is the estimated image of size m×n.

The Peak Signal-to-Noise Ratio (PSNR) is defined as a ratio between the maximum possible power of a signal and the noise power that affects the fidelity of its representation. PSNR is usually expressed in terms of the logarithmic decibel scale. It is most easily defined via the mean squared error (MSE).

$$PSNR = 10\log_{10}(\frac{peakval^2}{MSE})$$

Where maximum possible pixel value of the image when the pixels are represented using 8 bits per sample, this is 255.

B. SSIM

The SSIM is an index that measures the similarity between two images. The Structural Similarity (SSIM) Index quality assessment index is based on the computation of three terms, namely the luminance term, the contrast term and the structural term. The overall index is a multiplicative combination of the three terms.

$$SSIM(x,y) = [I(x,y)]^{\alpha} \cdot [c(x,y)]^{\beta} \cdot [s(x,y)]^{\gamma}$$

$$I(x,y) = \frac{2\mu_x\mu_y + C_1}{\mu_x^2 + \mu_y^2 + C_1},$$

$$c(x,y) = \frac{2\sigma_x\sigma_y + C_1}{\sigma_x^2 + \sigma_y^2 + C_1},$$

$$s(x,y) = \frac{\sigma_{xy} + C_3}{\sigma_x\sigma_y + C_3}$$

Where, μ_x, μ_y, σ_x, σ_y, and σ_{xy} are the local means, standard deviations, and cross-covariance for images x, y. If $\alpha = \beta = \gamma = 1$ (the default for Exponents), and $C_3 = C_2/2$ (default selection of C3) the index simplifies to:

$$SSIM(x,y) = \frac{(2\mu_x\mu_y + C_1)(2\mu_x\mu_y + C_2)}{(\mu_x^2 + \mu_y^2 + C_1)(\sigma_x^2 + \sigma_y^2 + C_2)}$$

Where μ_x and μ_y are averages of x and y respectively and σ_x and σ_y are variance of x and y respectively and σ_{xy} is the covariance between x and y.C_1 and C_2 are two variables that stabilize the division with weak denominator.

Table 1 PSNR in dB for different filtering methods

Diff Img	Noi var.	Lee	Frost	Kuan	SRAD
Abdomen img 1	0.02	28.9393	30.4054	31.3861	28.8662
	0.04	25.9045	30.2536	30.5801	25.8481
	0.06	24.1379	30.1206	29.9000	24.1054
	0.08	22.8767	29.9292	29.3202	22.8397
	0.1	21.9191	29.7639	28.8264	21.8510
	0.2	18.9110	28.8953	26.9389	18.9059
Brest img 1	0.02	28.7915	30.3282	31.9218	30.9979
	0.04	25.7770	30.1106	30.9933	30.7706
	0.06	24.0392	29.9858	30.3009	30.3559
	0.08	22.7952	29.7753	29.5880	30.1372
	0.1	21.8149	29.6454	29.1093	29.8801
	0.2	18.7781	28.8384	27.0745	28.6075
Carotid artery img 1	0.02	27.3038	27.3038	24.0238	27.9175
	0.04	24.2577	24.2577	23.4693	27.6612
	0.06	22.4366	22.4366	23.3624	27.2165
	0.08	21.1922	21.1922	23.0207	26.8999
	0.1	20.2618	20.2618	23.0932	26.7823
	0.2	17.2995	17.2995	22.2671	25.6927
Kidney img 1	0.02	28.7915	30.3282	31.9218	30.9979
	0.04	25.7770	30.1106	30.9933	30.7706
	0.06	24.0392	29.9858	30.3009	30.3559
	0.08	22.7952	29.7753	29.5880	30.1372
	0.1	21.8149	29.6454	29.1093	29.8801
	0.2	18.7781	28.8384	27.0745	28.6075

Table 2 SSIM for different filtering methods

Diff Img	Noi var.	Lee	Frost	Kuan	SRAD
A 1	0.02	0.8272	0.8016	0.8536	0.8264
	0.04	0.7520	0.8007	0.8317	0.7507
	0.06	0.7069	0.7987	0.8140	0.7080
	0.08	0.6777	0.7961	0.7984	0.6773
	0.1	0.6543	0.7933	0.7859	0.6545
	0.2	0.5958	0.7786	0.7362	0.5949
B 1	0.02	0.7617	0.8062	0.8695	0.8268
	0.04	0.6469	0.8031	0.8395	0.8212
	0.06	0.5756	0.7989	0.8141	0.8167
	0.08	0.5250	0.7961	0.7908	0.8096
	0.1	0.4871	0.7916	0.7729	0.8046
	0.2	0.3830	0.7676	0.6915	0.7774
C 1	0.02	0.5749	0.5749	0.8680	0.8324
	0.04	0.4500	0.4500	0.8374	0.8288
	0.06	0.3756	0.3756	0.8087	0.8207
	0.08	0.3236	0.3236	0.7880	0.8150
	0.1	0.2900	0.2900	0.7650	0.8134
	0.2	0.1883	0.1883	0.6699	0.7879
K 1	0.02	0.7617	0.8062	0.8695	0.8268
	0.04	0.6469	0.8031	0.8395	0.8212
	0.06	0.5756	0.7989	0.8141	0.8167
	0.08	0.5250	0.7961	0.7908	0.8096
	0.1	0.4871	0.7916	0.7729	0.8046
	0.2	0.3830	0.7676	0.6915	0.7774

VI. CONCLUSION

Diagnosis using ultrasound images is difficult because of the speckle noise which hampers the prediction and the extraction of fine details from the image. In this paper we described various existing filtering techniques to reduce this speckle noise and made comparison by using different ultrasound images of abdomen, brest, carotid artery and kidney images. From the outputs of the various filters, it can be seen that local statistics filter techniques were ineffective in “edge preservation” and “feature preservation”. The SRAD filter succeeded in preserving and enhancing edges and it gives best result for any ultrasound images.

Acknowledgment

The author would like to acknowledge Dr. Umesh Udapudi from Udapudi Clinic who has provided real ultrasound kidney images and Dr. Mishra for providing real ultrasound abdomen, brest and carotid artery images for these research work.

References

[1] Goodman, Joseph W. "Some fundamental properties of speckle." JOSA 66, Vol. no. 11, pp. 1145-1150 , (1976).J. Clerk Maxwell, A Treatise on Electricity and Magnetism, 3rd ed., vol. 2. Oxford: Clarendon, 1892, pp.68-73.

[2] Chan, Vincent, and Anahi Perlas. “Basics of ultrasound imaging.” Springer journal on Atlas of Ultrasound-Guided Procedures in Interventional Pain Management, pp. 13-19, (2011).

[3] Y. Yu, S.T. Acton, “Speckle reducing anisotropic diffusion.”IEEE Trans.on Image Process, Vol. 11 (no.11), pp. 1260–1270, (2002).

[4] Aja-Fernández, Santiago, and Carlos Alberola-López. "On the estimation of the coefficient of variation for anisotropic diffusion speckle filtering." *Image Processing, IEEE Transactions on* 15, no. 9,pp. 2694-2701, (2006).

[5] Mateo, Juan L., and Antonio Fernández-Caballero. "Finding out general tendencies in speckle noise reduction in ultrasound images." Expert Systems with Applications 36, no. 4 , pp. 7786-7797, (2009).M. Young, The Technical Writer's Handbook. Mill Valley, CA: University Science, 1989.

[6] Perona, Pietro, and Jitendra Malik. "Scale-space and edge detection using anisotropic diffusion." Pattern Analysis and Machine Intelligence, IEEE Transactions on 12, no. 7,pp. 629-639, (1990).

[7] J. S. Lee, "Digital image enhancement and noise filtering by using local statistics," IEEE Trans. Pattern Anal. Machine Intell., vol. PAM1-2,
1980.

[8] V. S. Frost, J. A. Stiles, K. S. Shanmugan, and J. C. Holtzman, "A model for radar images and its application to adaptive digital filtering of multiplicative noise," IEEE Trans. Pattern Anal. Machine Intell., vol. PAMI-4, pp. 157–165, 1982.

[9] D. T. Kuan, A. A. Sawchuk, T. C. Strand, and P. Chavel, "Adaptive restoration of images with speckle," IEEE Trans. Acoust., Speech, Signal Processing, vol. ASSP-35, pp. 373–383, 1987

[10] K.V. Devarapu, Subrahmanyam Murala, Vinod Kumar, Denoising of ultrasound images using curvelet transform, Int.Conf.Comput. Autom.Eng.3, pp. 447–451,(Feb26-28) (2010).

[11] Elamvazuthi, Irraivan, Muhammad Luqman Bin Muhd Zain, and K. M. Begam. "Despeckling of ultrasound images of bone fracture using multiple filtering algorithms." *Elsevier journal on Mathematical and Computer Modelling,* Vol.57 (no. 1), pp. 152-168, (2013).

[12] Bama, S., and D. Selvathi. "Despeckling of medical ultrasound kidney images in the curvelet domain using diffusion filtering and MAP estimation." *Elsevier journal on Signal Processing,* No.103, pp. 230-241, (2014).

[13] Zhang, Ju, Chen Wang, and Yun Cheng. "Comparison of despeckle filters for breast ultrasound images." *Springer journal on Circuits, Systems, and Signal Processing*, pp. 1-24, (2014).

[14] Loizou, Christos P., Constantinos S. Pattichis, Christodoulos I. Christodoulou, Robert SH Istepanian, Marios Pantziaris, and Andrew Nicolaides. "Comparative evaluation of despeckle filtering in ultrasound imaging of the carotid artery." *IEEE Transactions on Ultrasonics, Ferroelectrics and Frequency Control,* Vol. 52 (no. 10), pp.1653-1669, (2005).

[15] Mateo, Juan L., and Antonio Fernández-Caballero. "Finding out general tendencies in speckle noise reduction in ultrasound images." *Elsevier journal on Expert Systems with Applications,* Vol.36 (no. 4), pp. 7786-7797, (2009).

[16] Park, Jihoon, Jin Bum Kang, Jin Ho Chang, and Yangmo Yoo. "Speckle reduction techniques in medical ultrasound imaging." *Springer journal on Biomedical Engineering Letters,* Vol. 4 (no. 1) pp.32-40.

[17] R.C. Gonzalez, "Digital Image Processing", Pearson, 2009.

[18] Christos P. Loizou, Constantinos S. Pattichis, "Despeckle Filtering Algorithms and Software and Software for Ultrasound Imaging", Morgan and Claypool Publishers, 2008.